The 61st Fujihara Seminar: Progress in Solar / Stellar Physics with Helio- and Asteroseismology
ASP Conference Series, Vol. 462
H. Shibahashi, M. Takata, and A. E. Lynas-Gray, eds.

A Determination of High-degree Mode Parameters Based on MDI Observations

Sylvain G. Korzennik,[1] M. C. Rabello-Soares,[2] J. Schou,[2] and T. P. Larson[2]

[1]*Harvard-Smithsonian Center for Astrophysics, Cambridge, MA 02138, USA*

[2]*Stanford University, Stanford, CA 94305, USA*

Abstract. We present the best to date determination of high-degree mode parameters obtained from a ninety day long time series of full-disk full-resolution Michelson Doppler Imager (MDI) Dopplergrams. These Dopplergrams were decomposed using our best estimate of the image scale and the known components of MDI's image distortion. The spherical harmonic decomposition was carried out up to $\ell = 1000$, and a high-order sine multi-taper power spectrum estimator was used to generate power spectra. These power spectra were fitted for all degrees and all azimuthal orders, for $100 \leq \ell \leq 1000$, and for all radial orders with substantial amplitude, generating some 6×10^6 estimates of ridge frequencies, line-widths, amplitudes and asymmetries. We used a sophisticated forward modeling of the mode to ridge blending, to recover the best possible estimate of the underlying mode characteristics.

1. Introduction

The inclusion of accurate high-degree modes (i.e., $300 \leq \ell \leq 1000$) has the potential to improve dramatically inferences of the solar stratification and its dynamics in the outermost 2 to 3% of the Sun [see, for examples, Korzennik & Eff-Darwich (1999), Rabello-Soares et al. (2000)]. Unfortunately, the determination of the characteristics of the high-degree modes (i.e., their frequency, line-width, asymmetry and amplitude), remained, over the past two decades, a challenging task [see Korzennik (1990), Korzennik et al. (2004), Rabello-Soares et al. (2008), and references therein]. Indeed, at high degrees, individual modes blend into ridges, causing the individual mode characteristics to be masked by the ridge. The ridge frequency, for instance, is not the target mode frequency, but in fact a value offset by a significant amount.

2. Observations, Data Analysis, and Correction Methodology

The MDI instrument, launched in 1995, is on board the Solar and Heliospheric Observatory (SOHO) spacecraft that orbits the L1 Lagrangian point (Scherrer et al. 1995). While MDI took high resolution full-disk images, limited telemetry resulted in transmitting only binned data. But during limited time periods and nearly each year, NASA's Deep Space Network provided additional band-width to download unbinned images. The data we analyzed were acquired during the 2001 epoch when unbinned Dopplergrams are available for nearly 90 days of continuous observations at a high duty cycle.

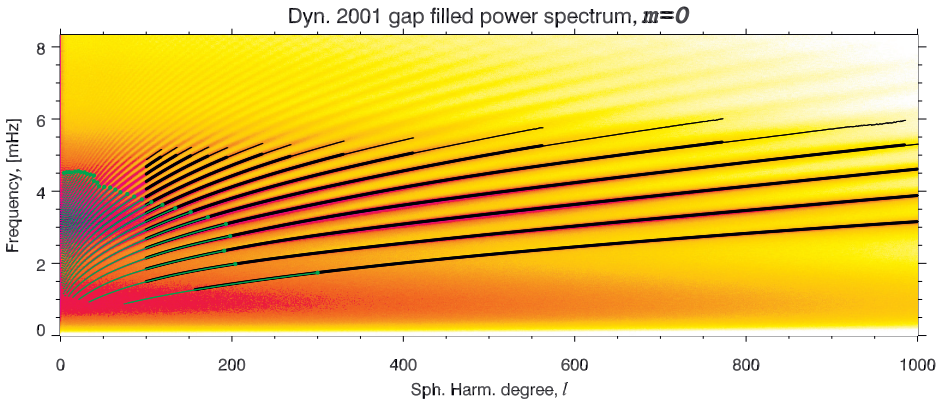

Figure 1. Dynamics 2001 power spectrum (zonal, $m = 0$), computed from gap-filled time series. The range of the ridge fitting is indicated by the black dots, while mode frequencies determined at low and intermediate degrees are indicated as green dots.

The MDI Dopplergrams analyzed for the study presented here were spatially decomposed into spherical harmonics, using an improved decomposition that incorporates our best knowledge of the instrumental image distortion. Korzennik et al. (2004) have described in minute detail the two components of this distortion. The resulting time series of spherical harmonic coefficients were gap filled, producing a 259,200 minutes long time series with a fill factor of 97.0% (95.8% prior to gap filling). Since the ridges at high degrees have large widths, there is no need for high spectral resolution. Therefore, we reduced the realization noise by using a high-order ($N = 61$) sine multi-taper power spectrum estimator, resulting in an effective spectral resolution of 7.8 μHz.

We were able to fit ridges down to $\ell = 100$, producing an overlap between mode and ridge fitting covering $100 \leq \ell \leq 300$ for the f-modes and $100 \leq \ell \leq 200$ for the p-modes. Figure 1 shows the *Dynamics* 2001 power spectrum for the zonal modes ($m = 0$) and the extent in the $\ell - \nu$ plane of the ridge and mode fitting. The ridge fitting was carried out between $\ell = 100$ and 1000 for all m, generating in excess of 6×10^6 multiplets (ℓ, n, m), corresponding to some 6×10^3 singlets (ℓ, n).

The methodology we used to recover mode characteristics from ridge fitting consists in modeling in detail the contribution of all the modes to the ridge. This model is then used to establish a correspondence between the ridge characteristics and the input mode characteristics (see Korzennik et al. 2004; Rabello-Soares et al. 2008). We recently improved the methodology as follows: (1) we fine-tuned the input parameters of the model, (2) iterated some model input parameters to produce an improved agreement with observation and (3) we ran perturbed models to get a measure of the model's sensitivity to its input parameters.

3. Results

Figure 2 compares the frequencies (singlets) between corrected ridge frequencies and mode frequencies for the $100 \leq \ell \leq 300$ overlap. The figure also shows the odd Clebsch-Gordan coefficients used to parametrize the frequency splittings, for all de-

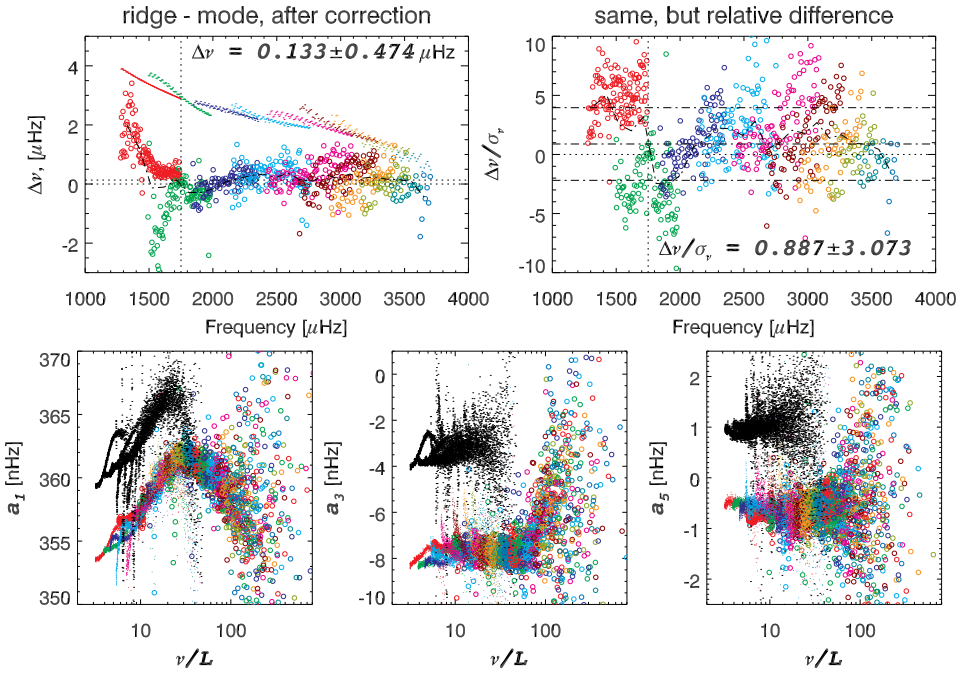

Figure 2. Top panels: differences between corrected ridge frequencies and mode frequencies, and relative differences, i.e., differences divided by the ridge fitting uncertainties, for the overlapping ℓ range (shown in Fig. 1). The dots in the left panel are the ridge to mode frequency corrections. Bottom panels: comparison of odd Clebsch-Gordan coefficients, as a function of ν/L. The circles are values derived from fitting resolved modes, the black dots correspond to ridge fitting, while the filled circles are the resulting values after applying the ridge to mode frequency correction. The color coding corresponds to the radial order, n.

grees, before and after correcting the ridge frequencies. The figures show the agreement between the corrected ridge frequencies and the resolved mode measurements (singlets), but for $\nu \geq 1750\,\mu$Hz, with a scaled differences mean and RMS of $\Delta\nu/\sigma = 0.89 \pm 3.1$. The Clebsch-Gordan coefficients derived from the corrected ridge frequencies are consistent with determinations from resolved modes, but for some features at the low-ℓ ends of some ridges.

Figure 3 shows how well our model reproduces the variation of the amplitude, FWHM, and asymmetry of the ridge with m. Note that the mode values used as input to the model are constant with m. Our model prediction of the ridge amplitude variation with m is a stringent test of the adequacy of the leakage matrix, and we fail to match in detail the observations, especially for the very high degrees. This must have some effect on the other measured characteristics (ν, Γ, α). We suspect that our limited knowledge of MDI's PSF is the primary culprit of this mismatch.

Acknowledgments. The Solar Oscillations Investigation (SOI) involving MDI is supported by NASA grant NNG05GH14G at Stanford University. SOHO is a mission of international cooperation between ESA and NASA. SGK is supported by NASA grant NNX09AB15G.

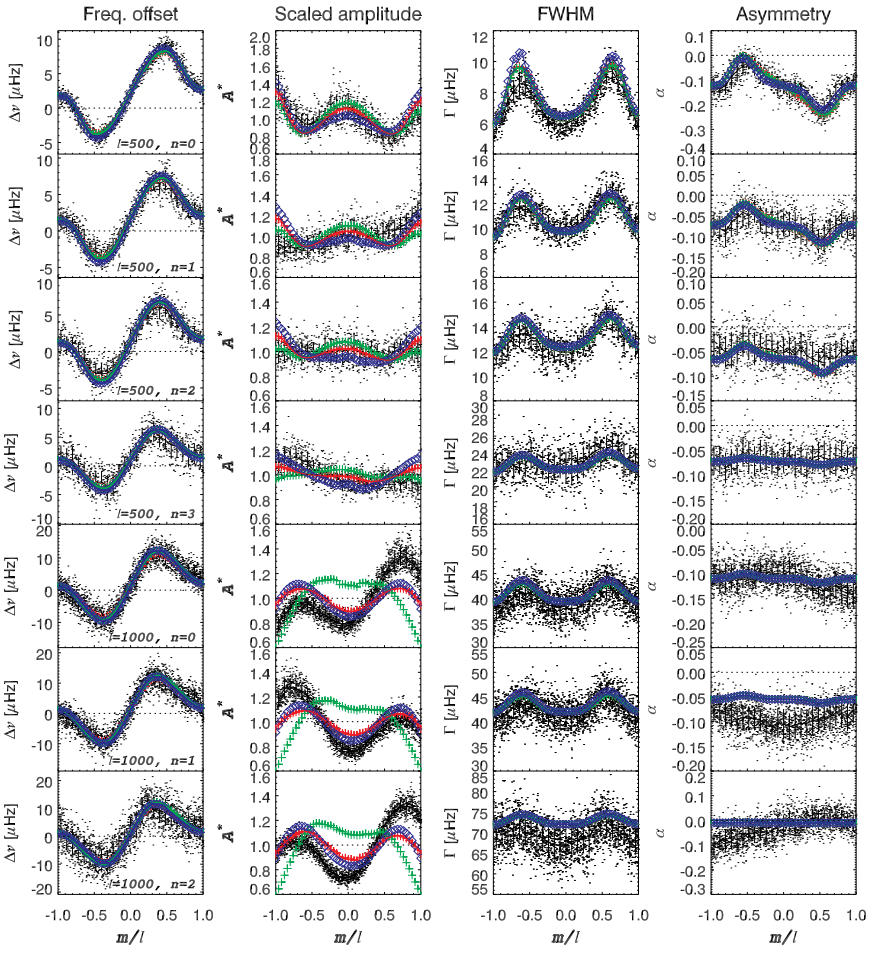

Figure 3. Comparison of model and measured ridge properties, as a function of m/ℓ, (for ℓ=500, n=0-3 and ℓ=100, n=0-2). Left to right: ridge to mode frequency offset, scaled amplitude [divided by $1 + (m/\ell)^2$], FWHM and asymmetry. The dots are measured values with black lines corresponding to binned values. The red curves show the model values, using the MDI-team leakage matrix. The green and blue curves correspond to an independent computation of the leakage matrix, with or without the inclusion of a PSF. Note the good agreement of the variation with m but for the amplitude, while the underlying mode width asymmetry and amplitude are independent of m.

References

Korzennik, S. G. 1990, Ph.D. Thesis, University of California, Los Angeles

Korzennik, S. G., & Eff-Darwich, A. 1999, SOHO-9 Workshop on Helioseismic Diagnostics of Solar Convection and Activity, 9

Korzennik, S. G., Rabello-Soares, M. C., & Schou, J. 2004, ApJ, 602, 481

Rabello-Soares, M. C., Basu, S., Christensen-Dalsgaard, J., & Di Mauro, M. P. 2000, Solar Phys., 193, 345

Rabello-Soares, M. C., Korzennik, S. G., & Schou, J. 2008, Solar Phys., 251, 197

Scherrer, P. H., Bogart, R. S., Bush, R. I., et al. 1995, Solar Phys., 162, 129